WEP Warwick Evans Publishing

International Journal of Materials Science and Technology Studies

ISSN: 3006-7693 (Print), ISSN: 3006-3744 (Online) | Volume 4, Number 2, Year 2025
DOI: https://doi.org/10.62051/ijmsts.v4n2.01
Journal homepage: https://wepub.org/index.php/IJMSTS/index

Preparation and Properties Study of Magnesium Potassium Phosphate-based Carbon-Solidifying Cementitious Materials

Haijie Li, Ziru Guo, Shiying Chen *

College of Resources and Environment, Henan Polytechnic University, Jiaozuo 454003, China

ABSTRACT

This study systematically investigates the effects of the Mg/P ratio, water-to-binder ratio, pre-curing time, and mineral admixtures on the performance of magnesium potassium phosphate cement (MKPC) as a carbon sequestration material. The results demonstrate that an Mg/P ratio of 3:1 provides the highest compressive strength under both ambient and carbonation curing conditions, with unreacted MgO serving as an additional magnesium source during carbonation. A water-to-binder ratio of 0.25 promotes sufficient hydration and a stable pore structure, leading to enhanced mechanical properties. The incorporation of carbide slag (CCR) notably improved the carbonation rate compared to the control group, while metakaolin contributed to the formation of binding phases that refined the microstructure. Pre-curing duration significantly influenced the reaction kinetics and diffusion of CO_2, with both insufficient and excessive durations negatively affecting carbonation efficiency. The findings provide important insights into the design of high-performance MKPC-based materials for carbon capture and storage.

KEYWORDS

Magnesium Potassium Phosphate; Calcium Carbide Sludge; Carbonization

1. INTRODUCTION

Magnesium phosphate cement (MPC) is a type of chemically bonded ceramic formed through the acid–base reaction between calcined magnesia and a soluble acid phosphate. Soudée et al. [1] proposed that the crystallization of $NH_4MgPO_4·6H_2O$ follows a mechanism of local chemical reaction, wherein the wetted surface of MgO forms $Mg(H_2O)_6^{2+}$, which subsequently reacts with PO_4^{3-} and NH_4^+ to form $NH_4MgPO_4·6H_2O$ crystals. Wagh et al. [2] suggested that the crystallization of $MgKPO_4·6H_2O$ occurs via heterogeneous nucleation. According to this theory, MgO first dissolves in the phosphate solution to release Mg^{2+}, which complexes with water molecules to form an aquo-complex $[Mg(H_2O)_6]^{2+}$. These complexes then gradually react with PO_4^{3-} and K^+ to crystallize into $KMgPO_4·6H_2O$, resulting in the setting and hardening of the cement paste.

Mo [3] proposed that in an acidic environment, the surface of MgO particles is directly protonated by H^+ ions to form Mg^{2+}. However, a number of researchers argue that the protonation of MgO requires the involvement of water molecules [4–6]. Specifically, the MgO surface sequentially adsorbs one and two water molecules, undergoing hydration to form $Mg(OH)_2$, which then detaches from the surface and dissociates into Mg^{2+} and OH^-. The OH^- immediately reacts with H^+ in the solution, leading to an increase in pH. After the release of Mg^{2+}, magnesium potassium phosphate (MKP) begins to form and precipitate [7]. Initially, Mg^{2+} in the solution coordinates with six water molecules to form $[Mg(H_2O)_6]^{2+}$, which adsorbs onto the surface of MgO particles. It then polymerizes with K^+ and PO_4^{3-} in the solution to form a dense multi-component gel product.

MPC mortar primarily consists of magnesia and phosphate hydrates. Studies have shown that excess MgO accelerates the reaction rate and shortens the setting time. However, as the Mg/P ratio continues to increase, a significant amount of unreacted MgO remains in the cementitious system. The chemical composition of magnesium slag is presented in Table 1-1.

Table 1-1. Chemical Composition of Magnesium Slag (wt%)

Component	MgO	SiO_2	Sb_2O_2	Bi_2O_3	Fe_2O_3	CaO	Al_2O_3	Others
Content (wt%)	74.50	18.69	2.14	1.22	1.21	0.528	0.449	1.213

When MgO particles come into contact with water, MgO acts as an electron donor, releasing surface-adsorbed OH^- anions and introducing positively charged Mg^{2+} and OH^- ions into the solution [8, 9]. As the ion concentration reaches a supersaturated state, magnesium hydroxide ($Mg(OH)_2$) begins to precipitate on the surface of the MgO particles. The exposed brucite ($Mg(OH)_2$) layer can subsequently react with CO_2 and H^+, leading to the formation of magnesium bicarbonate solution, which may further precipitate as hydrated magnesium carbonate (HMC). These processes can be represented by the following equations:

$$Mg(OH)_2(s)+2CO_2(aq)\rightarrow Mg^{2+}+2HCO^{3-}$$

$$Mg(OH)_2(s)+2H^+\rightarrow Mg^{2+}+2H^2O$$

$$Mg^{2+}+2HCO^{3-}+xH_2O\rightarrow MgCO_3\cdot xH_2O+H^++HCO^{3-}$$

Various types of hydrated magnesium carbonates (HMCs) exhibit substantial binding affinity among themselves [10], as seen in phases such as nesquehonite ($MgCO_3\cdot 3H_2O$), hydrotalcite ($Mg_5(CO_3)_4(OH)_2\cdot 4H_2O$),basic magnesium carbonate ($Mg_5(CO_3)_4(OH)_2\cdot 5H_2O$), and artinite ($Mg_2(OH)_2CO_3\cdot 3H_2O$).

Industrial by-product gypsum and carbide slag are both solid wastes rich in calcium. The carbonation method utilizes industrial by-product gypsum as the source of Ca^{2+} ions. By introducing CO_2 into the reaction system, carbonate ions (CO_3^{2-}) are generated, which then combine with calcium ions to form a precipitate of $CaCO_3$. The reaction can be represented by the following equation:

$$CaO+CO_2 = CaCO_3$$

$$CaO\cdot SiO_2 + CO_2 = CaCO3 + SiO_2$$

In summary, the utilization of magnesium slag, industrial by-product gypsum, and carbide slag for the preparation of cementitious materials demonstrates considerable theoretical feasibility for carbonation. Further research should focus on optimizing the mix design and carbonation conditions to achieve optimal performance.

2. RESULTS AND DISCUSSION

To determine the carbonation conditions, an experimental scheme was designed in which magnesium slag, potassium dihydrogen phosphate, and various mineral admixtures were proportioned at different ratios. The raw materials for the porous magnesium phosphate cement-based composites were precisely weighed according to the specified mix proportions. The dry components were first combined in a mixing pot and blended uniformly using a cement mortar mixer at low speed for 120 s. Subsequently, tap water was added in accordance with the designated water-to-binder ratio and

mixed until a homogeneous paste was achieved. The resulting paste was then cast into 40 mm × 40 mm × 160 mm triple-gang molds in accordance with GB/T 17671-2021 “Test method for cement mortar strength”. To eliminate entrapped air and ensure uniformity, the molds were vibrated on a shaking table. Cylindrical specimens were prepared for both compressive and flexural strength tests.Ambient-cured group: specimens were directly placed in an environment maintained at 20 ± 2 °C and 60 ± 2% RH until the testing ages.CO_2-cured group: following demolding, specimens were transferred into a carbonation chamber with conditions of 20 ± 2 °C, 60 ± 2% RH, and 20% CO_2 concentration for 24 hours of mineral carbonation. Afterwards, they were moved to the same ambient conditions (20 ± 2 °C, 60 ± 2% RH) for continued curing until testing.

2.1. Effect of Mg/P Ratio on the Properties of Cementitious Materials

The influence of the Mg/P ratio on the properties of magnesium potassium phosphate cement was investigated under both standard ambient curing and carbonation curing conditions, while maintaining a constant water-to-binder ratio. The detailed experimental plan is provided in Table 3-1.

Table 3-1. Experimental Design for Investigating the Effect of Mg/P Ratio on the Properties of Cementitious Materials

Sample ID	Mix Proportions and Curing Methods		
	M/P	W/S	Curing Regime
A1-N	1:1	0.4	Curing Regime
A2-N	2:1	0.4	
A3-N	3:1	0.4	
A4-N	4:1	0.4	
A5-N	5:1	0.4	
A6-N	6:1	0.4	
A7-N	7:1	0.4	
A8-N	8:1	0.4	
A9-N	9:1	0.4	
A1-C	1:1	0.4	Curing Regime
A2-C	2:1	0.4	
A3-C	3:1	0.4	
A4-C	4:1	0.4	
A5-C	5:1	0.4	
A6-C	6:1	0.4	
A7-C	7:1	0.4	
A8-C	8:1	0.4	
A9-C	9:1	0.4	

2.1.1. Analysis of Mechanical Properties

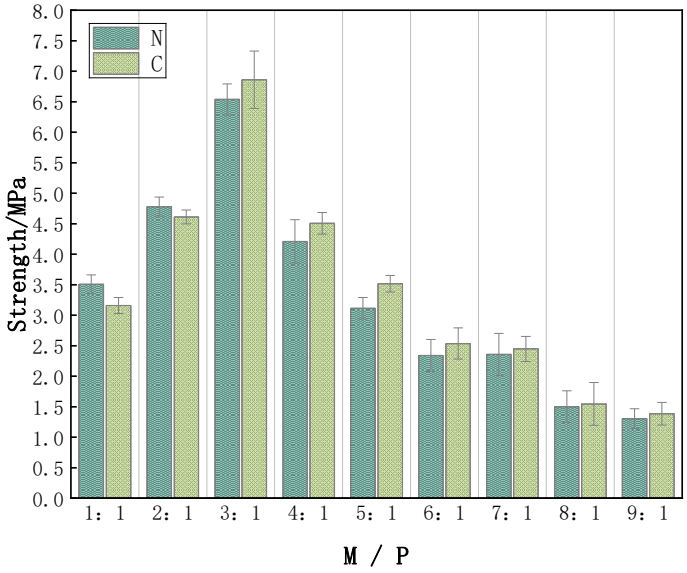

Figure 3-1. Effect of Mg/P Ratio on the Mechanical Properties of Cementitious Materials

As the Mg/P ratio increased, the compressive strength of specimens under both curing regimes initially rose and then declined. According to the theoretical stoichiometric ratio, a complete reaction requires Mg/P = 1:1 [11]. Under ambient curing conditions, when the Mg/P ratio was 1:1 and 2:1, the compressive strengths were 3.51 MPa and 4.78 MPa, respectively. The lower strength is attributed to the incomplete reaction of industrial-grade MgO, which is not fully reactive, resulting in reduced formation of $MgKPO_4 \cdot 6H_2O$ (MKP) and weaker cementation. At an Mg/P ratio of 3:1, the strength increased significantly to 6.64 MPa. At this ratio, the system consists of both hydration products and unreacted raw materials. Compared to KH_2PO_4, MgO calcined at 1450 °C possesses a denser microstructure. During its hydration, MKP crystals form on the surface of MgO particles. The residual MgO, which has a higher hardness than MKP, contributes to enhancing the mechanical properties of the specimen. However, experimental data indicate that when the Mg/P ratio exceeds 4:1, the compressive strength begins to decrease. This decline occurs because the higher Mg/P ratio reduces the content of KH_2PO_4. Insufficient KH_2PO_4 interrupts the continuous supply of PO_4^{3-} and K^+ ions, leading to an insufficient volume fraction of the binding phase (MKP). As a result, an effective cohesive network cannot be formed, ultimately compromising the overall mechanical performance.

In contrast, under carbonation curing, the strength of specimens with Mg/P ratios between 1:1 and 2:1 slightly decreased compared to those under ambient curing. This suggests that the conversion of residual reactants into salts under CO_2 exposure may cause a certain loss of strength. When the Mg/P ratio ranged from 3:1 to 7:1, strength improvement was observed. However, beyond an Mg/P of 7:1, strength again declined. This behavior can be explained by the fact that at moderate Mg/P ratios, unreacted MgO not only supplies additional Mg^{2+} for continued reaction but also generates hydrated magnesium carbonate (HMC) in the CO_2-rich environment, which densifies the matrix by pore filling [12]. In contrast, excessively high Mg/P ratios lead to an accumulation of inert MgO particles, forming weak interfaces and impeding the interconnection of hydration products. This results in a looser microstructure, an effect that is more pronounced under carbonation conditions.

2.1.2. XRD(M/P)

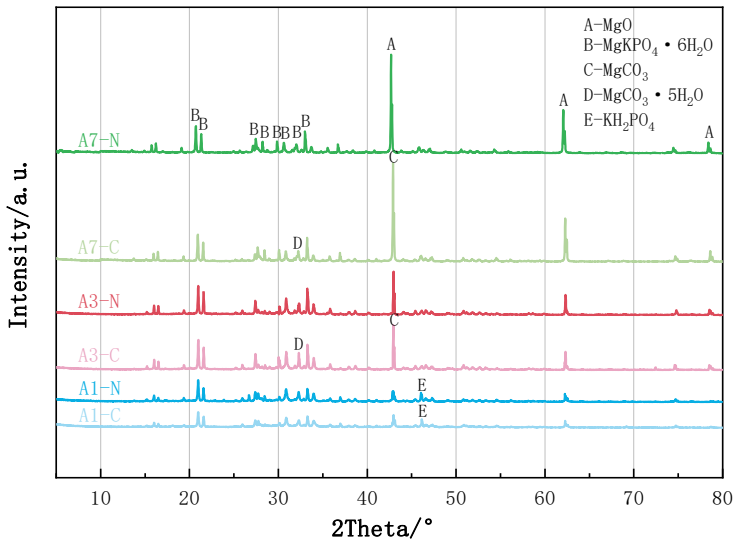

Figure 3-2. XRD Patterns of Specimens with Different Mg/P Ratios

As shown in Fig. 3-2, the diffraction peaks of MgO in samples A1-N and A1-C are significantly lower compared to other specimens. Meanwhile, a distinct diffraction peak of KH_2PO_4 is observed at $2\theta = 46.26°$, indicating the presence of unreacted KH_2PO_4 in the system. Due to its strong hygroscopicity, the residual KH_2PO_5 tends to absorb moisture, leading to the formation of liquid phases or softened interfaces, thereby reducing the overall compactness of the material. In comparison with sample A3-N, the unreacted MgO diffraction peaks in A7-N are noticeably more intense, accompanied by a reduction in the content of $MgKPO_4·6H_2O$. This observation correlates well with the decrease in compressive strength observed in these specimens. For the carbonation-cured samples A3-C and A7-C, overlapping diffraction peaks of residual MgO and magnesite ($MgCO_3$) are detected at $2\theta = 42.92°$, along with the presence of lansfordite ($MgCO_3·5H_2O$). These phases are not detected in sample A1-C, which may be attributed to differences in the reactivity of MgO under varying Mg/P conditions.

Furthermore, the content of $MgKPO_4·6H_2O$ in samples A3-C and A7-C is slightly higher than that in their ambient-cured counterparts (A3-N and A7-N). This finding is consistent with previous studies reporting the formation of additional MKP phases under carbonation conditions [13], suggesting that the CO_2 treatment promotes further reaction within the system.

2.1.3. SEM(M/P)

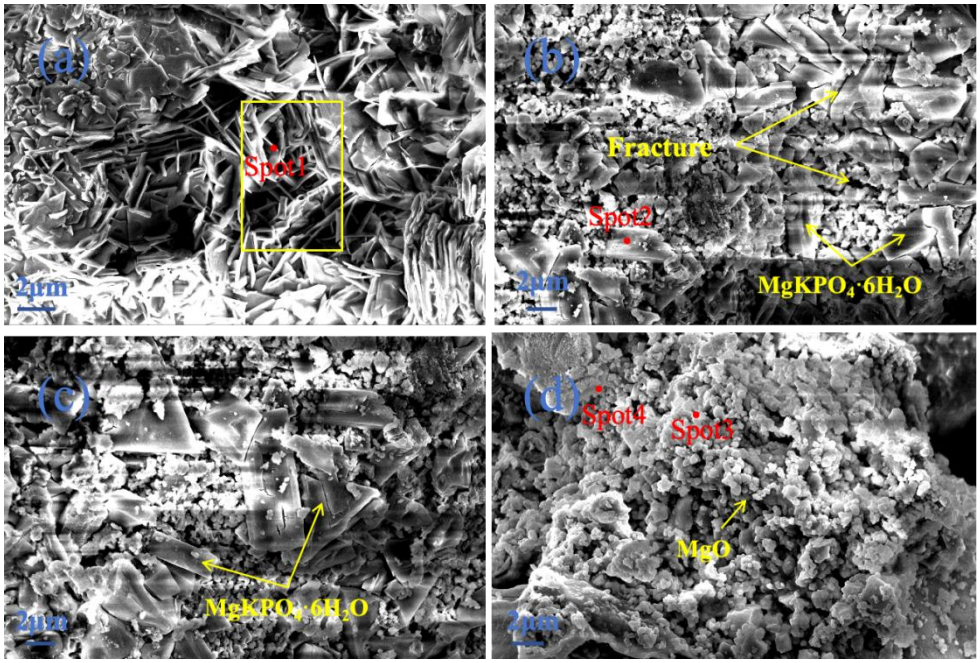

Figure 3-3. SEM images of (a) A1-N, (b) A3-N, (c) A3-C, and (d) A7-N specimensSEM

Figure 3-3 presents SEM images of specimens with Mg/P ratios of 1:1 (Fig. 3-3a) and 7:1 (Fig. 3-3d). In the sample with an Mg/P ratio of 1:1, needle-like crystals are observed. The excess KH_2PO_4 leads to a locally elevated concentration of PO_4^{3-}, promoting the preferential growth of MKP crystals along specific crystallographic planes. This morphology is consistent with the observed compressive strength performance. In contrast, the sample with an Mg/P ratio of 7:1 exhibits numerous unreacted MgO particles, which are dispersed in an isolated manner and display smooth surfaces. The high MgO content accelerates the setting process, potentially inducing greater internal stresses within the specimen. After solidification, increased microcracking is observed in high Mg/P ratio samples.SEM images of specimens with an Mg/P ratio of 3:1 under carbonation curing (Fig. 3-3c) and ambient curing (Fig. 3-3b) are also compared. The ambient-cured sample shows noticeable microcracks, unevenly distributed unreacted MgO particles, and multiple fissures. In comparison, the carbonation-cured specimen exhibits a denser structure and a more homogeneous overall morphology. This improvement is primarily attributed to the formation of hydrated magnesium carbonate (HMC) during carbonation, which effectively fills internal pores and thereby refines the microstructure.

2.1.4. EDS(M/P)

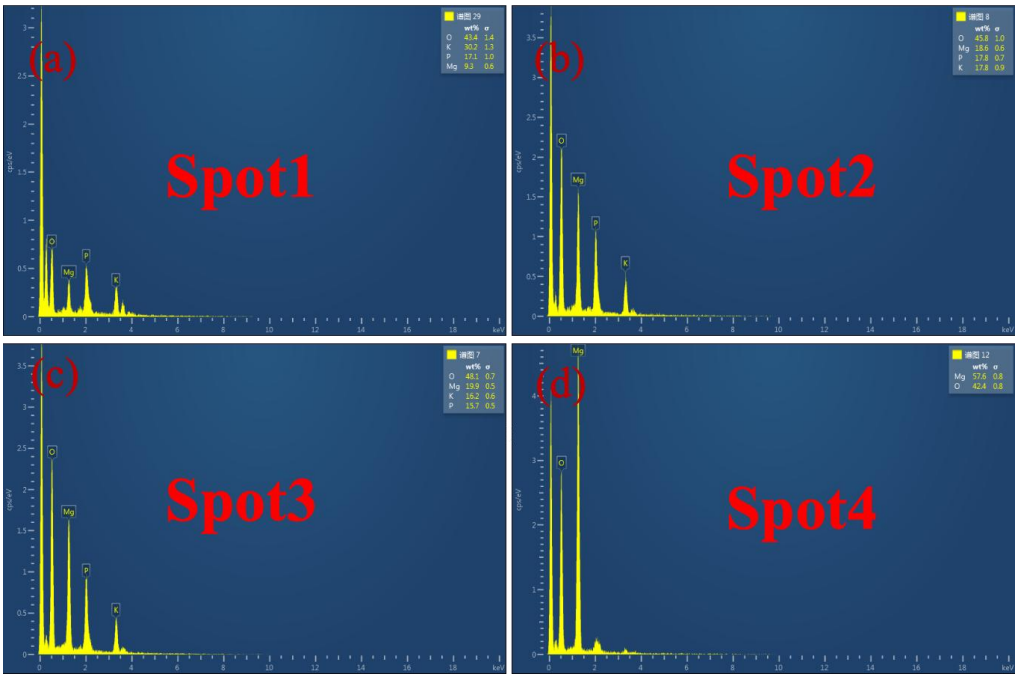

Figure 3-4. EDS elemental mappings of (a) A1-N, (b) A3-N, (c) A7-N, and (d) A7-N specimens

EDS analysis (Fig. 3-4) reveals distinct differences in the elemental distribution among samples with different mix proportions. In the specimen with an Mg/P ratio of 1:1 (Fig. 3-4a), the atomic ratio is O: Mg: K: P ≈ 1.44: 0.31: 1.00: 0.57, indicating a deficiency in Mg content and suggesting the presence of a significant amount of unreacted KH_2PO_4. For the sample with an Mg/P ratio of 3:1 (Fig. 3-4b), the atomic ratio is O: Mg: K: P ≈ 2.57: 1.04: 1.00: 1.00, which closely matches the theoretical elemental composition of MKP ($MgKPO_4 \cdot 6H_2O$). The characteristic peak positions are consistent with the standard reference pattern of struvite-type phases, confirming that the hydration product is indeed the MKP phase.

2.2. Effect of Water-to-Binder Ratio on the Properties of Cementitious Materials

Based on the optimal compressive strength mix proportion A-3 identified in Section 3-1, the water-to-binder ratio was varied to investigate its influence on the properties of magnesium potassium phosphate cement under both ambient curing and carbonation curing conditions. The experimental design is summarized in Table 3-2.

Table 3-2. Experimental Design for Investigating the Effect of Water-to-Binder Ratio on the Properties of Cementitious Materials

Sample ID	Mix Proportions and Curing Methods		
	M/P	W/S	Curing Regime
B1-N	3:1	0.15	Curing Regime
B2-N	3:1	0.20	
B3-N	3:1	0.25	
B4-N	3:1	0.30	
B5-N	3:1	0.35	
B6-N	3:1	0.40	
B7-N	3:1	0.45	
B8-N	3:1	0.50	
B1-C	3:1	0.15	Curing Regime
B2-C	3:1	0.20	
B3-C	3:1	0.25	
B4-C	3:1	0.30	
B5-C	3:1	0.35	
B6-C	3:1	0.40	
B7-C	3:1	0.45	
B8-C	3:1	0.50	

2.2.1. Analysis of Mechanical Properties

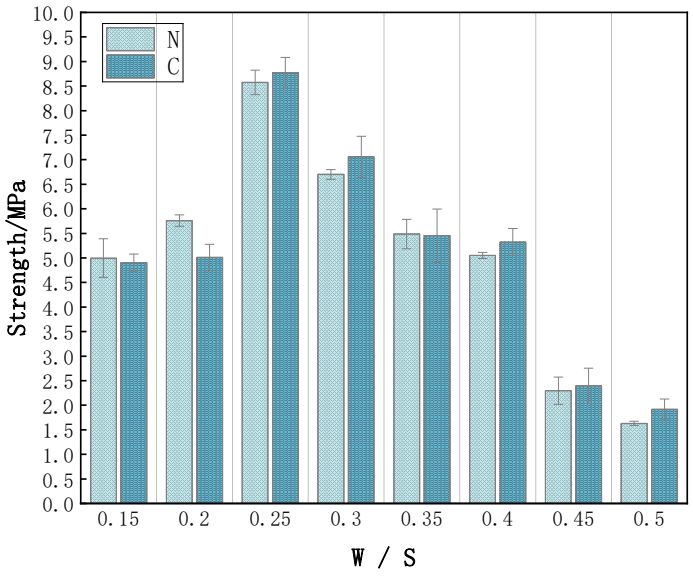

Figure 3-5. Effect of Water-to-Binder Ratio on Mechanical Properties of Cementitious Materials

Figure 3-5 illustrates the influence of the water-to-solid ratio (W/S) on the mechanical properties of the specimens. When the W/S ratio is 25% or lower, samples B1 and B2 exhibit poor compressive strength under both curing conditions. This is attributed to the rapid hydration reaction, which sharply reduces the water content in the system. Additionally, temperature rise during reaction accelerates water evaporation, leading to very short setting times. These factors collectively restrict sufficient ion diffusion and result in incomplete reactions, thereby reducing the amount of hydration products formed. When the W/S ratio exceeds 25%, excess water that does not participate in the chemical reaction remains in the paste as free water. During hardening, this water tends to form numerous unstable air pores, causing expansion and disrupting the continuous growth of cementitious products. This adversely affects the formation and integrity of the specimens. For instance, the compressive

strengths of B8-N and B8-C are only 19.01% and 21.84%, respectively, of those of B3-N and B3-C. Furthermore, specimens with high W/S ratios display a significant number of microcracks. According to Griffith's crack theory [14], materials with a high volume of pores exhibit higher stress concentration factors than those with fewer pores. A higher stress concentration factor corresponds to lower compressive strength. Thus, elevated W/S ratios lead to reduced packing density, increased stress concentration, and consequently, a further decline in compressive performance.

2.2.2. XRD (W/S)

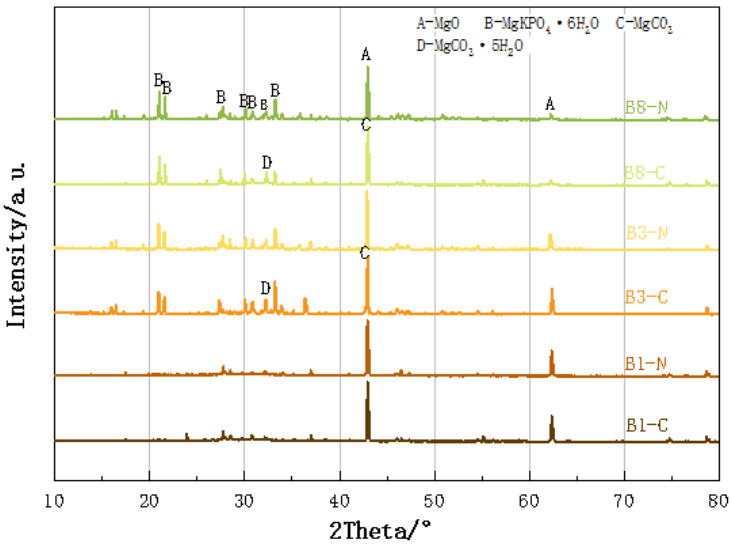

Figure 3-6. XRD Patterns of Specimens with Different Water-to-Binder Ratios

Figure 3-6 displays the XRD patterns of specimens with an Mg/P ratio of 3:1 at different water-to-solid (W/S) ratios. The phases in samples B3-N and B8-N consist primarily of MgO and $MgKPO_4 \cdot 6H_2O$, whereas in sample B1-N, the characteristic diffraction peaks of $MgKPO_4 \cdot 6H_2O$ are replaced by a broad hump, and unreacted MgO is also detected. This suggests that due to the low solubility of MgO, the excess MgO did not participate in the reaction to form crystalline phosphate phases. Instead, the hydration products in this system are predominantly amorphous.

In the XRD patterns of samples B3-N and B3-C, the main diffraction peaks correspond to the MKP phase and MgO, indicating that both hydration products and unreacted MgO persist even after the carbonation process. Additionally, diffraction peaks of magnesite ($MgCO_3$) and other carbonate phases, such as hydrated magnesium carbonates, are observed. This confirms the interaction between CO_2 from the carbonation chamber and the MKPC paste during the mineralization process.

2.3. Effect of Mineral Admixtures on the Properties of MKPC

The Mg/P and water-to-binder ratios were kept constant, and 10 wt% of different supplementary materials—Portland cement (P.O), carbide slag (CCR), ground granulated blast furnace slag (SL), metakaolin (MK), and fly ash (FA)—were individually incorporated into the base mixture. The specimens were pre-cured for 1, 3, and 7 days, followed by curing under both ambient and carbonation conditions. Their performance was compared with that of a control group (Ctrl) to investigate the effects of various admixtures and pre-curing durations on the properties of magnesium potassium phosphate cement-based materials. The detailed experimental plan is provided in Table 3-3.

Table 3-3. Experimental Design for Investigating the Effect of Mineral Admixtures on the Properties of Cementitious Materials

Group No.	Sample ID	Proportioning and maintenance			
		MKPC (g)	Admixture (g)	Pre-curing Time (days)	Curing Regime
MKP-Ctrl-N	1	1100	0	1d	Curing Regime
	3	1100	0	3d	
	7	1100	0	7d	
MKP-P.O-N	1	1000	110	1d	
	3	1000	110	3d	
	7	1000	110	7d	
MKP-CCR-N	1	1000	110	1d	
	3	1000	110	3d	
	7	1000	110	7d	
MKP-SL-N	1	1000	110	1d	
	3	1000	110	3d	
	7	1000	110	7d	
MKP-MK-N	1	1000	110	1d	
	3	1000	110	3d	
	7	1000	110	7d	
MKP-FA-N	1	1000	110	1d	
	3	1000	110	3d	
	7	1000	110	7d	
MKP-Ctrl-C	1	1100	0	1d	Curing Regime
	3	1100	0	3d	
	7	1100	0	7d	
MKP-P.O-C	1	1000	110	1d	
	3	1000	110	3d	
	7	1000	110	7d	
MKP-CCR-C	1	1000	110	1d	
	3	1000	110	3d	
	7	1000	110	7d	
MKP-SL-C	1	1000	110	1d	
	3	1000	110	3d	
	7	1000	110	7d	
MKP-MK-C	1	1000	110	1d	
	3	1000	110	3d	
	7	1000	110	7d	
MKP-FA-C	1	1000	110	1d	
	3	1000	110	3d	
	7	1000	110	7d	

2.3.1. Analysis of Mechanical Properties

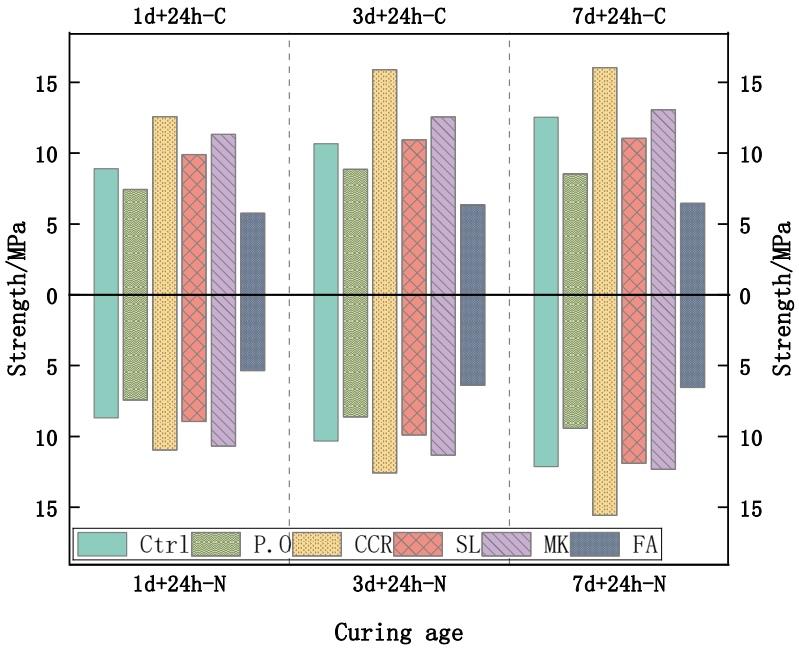

Figure 3-7. Compressive Performance of Specimens with Different Admixtures under Various Conditions

Figure 3-7 shows the compressive strength of MKPC specimens after 24 hours of ambient curing following pre-curing periods of 1, 3, and 7 days. For the control group (MKP-Ctrl-N), the compressive strength was 8.7 MPa at 1 day, increasing to 10.33 MPa and 12.13 MPa at 3 and 7 days, respectively. Specimens with slag (MKP-SL-N), Portland cement (MKP-P.O-N), and fly ash (MKP-FA-N) exhibited lower compressive strengths than the control at the same ages. In contrast, specimens with carbide slag (MKP-CCR-N) and metakaolin (MKP-MK-N) demonstrated improved performance, achieving strengths of 10.97 MPa / 10.70 MPa at 1 day, 12.57 MPa / 11.32 MPa at 3 days, and 15.57 MPa / 12.33 MPa at 7 days, respectively. The enhancement in MKP-CCR-N may be attributed to the calcium source in CCR reacting with PO_4^{3-} to form calcium phosphate compounds with lower solubility [15]. Additionally, the fine particle size of CCR contributes to pore filling, refining the microstructure and reducing internal defects, thereby directly increasing compressive strength. For MKP-MK-N, the improvement is likely due to the heat released during MKPC hydration activating the Al_2O_3 in metakaolin. The resulting Al^{3+} ions can react with PO_4^{3-} to form berlinite ($AlPO_4$) [16], which enhances the structural integrity and strength of the specimen.

Compared to ambient curing, the incorporation of 10 wt% P.O, SL, MK, or FA did not lead to significant changes in strength under carbonation curing. However, the MKP-CCR-C specimen pre-cured for 1, 3, and 7 days and then carbonated for 24 hours exhibited compressive strengths of 12.57 MPa, 15.89 MPa, and 16.04 MPa, respectively. These values represent an improvement over both MKP-Ctrl-N and MKP-CCR-N, with the highest strength observed after 3 days of pre-curing. This enhancement may be due to the higher reactivity of calcium-containing phases in CCR with CO_2 compared to magnesium-containing phases. The formation of $CaCO_3$ during carbonation fills pores and refines the microstructure of the blended system. Additionally, carbonation curing may promote further hydration in the cementitious system, leading to increased formation of hydration products [17].

2.3.2. Effect of Pre-curing Duration on Carbon Sequestration Capacity

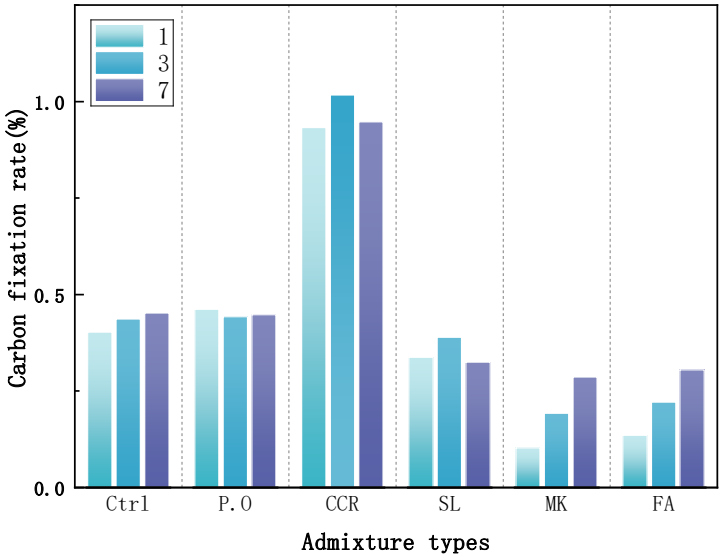

Figure 3-8. Carbonation Rates of Specimens with Different Admixtures under Carbonation Curing

The efficiency of the carbonation reaction is influenced by multiple factors, among which the pre-curing duration—defined as the time between sample preparation and exposure to a CO_2 environment—plays a critical role. As shown in Fig. 3-8, different admixtures exhibit varying carbon sequestration performances under identical carbonation conditions. The MKP-CCR-C specimen demonstrated the highest carbonation efficiency, with carbonation rates after 1, 3, and 7 days of pre-curing increasing by 131.84%, 133.25%, and 109.51%, respectively, compared to the MKP-Ctrl-C group. The pre-curing duration significantly affects the synchronicity between surface and internal reactions. After 1 day of pre-curing, rapid carbonation occurs at the surface, forming a dense shell that impedes CO_2 penetration to the unreacted calcium phases within the specimen. At 3 days of pre-curing, the reduction in free water content improves the diffusivity of CO_2, facilitating its ingress into the mixture and promoting the precipitation of $CaCO_3$. After 7 days of pre-curing, hydration products further fill the pores, resulting in a densified microstructure that limits CO_2 permeability and diffusion, ultimately leading to a encapsulation effect within the specimen.

2.3.3. XRD

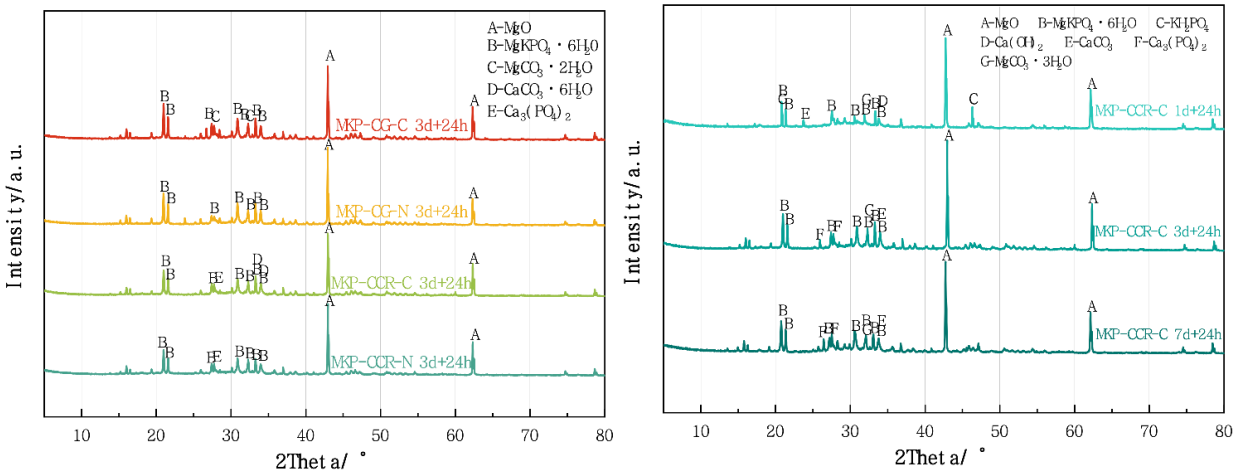

Figure 3-9. XRD patterns: (left) control group and 10 wt% CCR-blended specimen; (right) 10 wt% CCR-blended specimens pre-cured for 1, 3, and 7 days followed by 24 h carbonation

Figure 3-9 presents the X-ray diffraction (XRD) patterns of MKP-Ctrl and MKP-CCR blended specimens pre-cured for 3 days under both ambient and carbonation curing conditions. As shown in

Fig. 3-9 (left and right), distinct diffraction peaks corresponding to unreacted MgO and $MgKPO_4 \cdot 6H_2O$ are observed in all samples.

In both MKP-Ctrl-N and MKP-CCR-N specimens, hydrated magnesium carbonate (HMC) is identified, along with a reduction in the intensity of MgO peaks, indicating the occurrence of carbonation. The presence of $Ca_3(PO_4)_2$ in the MKP-CCR sample further explains its enhanced compressive strength.

Additionally, in the carbonation-cured MKP-CCR-C specimen (Fig. 3-9, right), $CaCO_3$ formed during carbonation is detected. After 1 day of pre-curing, clear diffraction peaks of dipotassium hydrogen phosphate (K_2HPO_4), unreacted MgO, and $Ca(OH)_2$ are visible. With extended pre-curing time, the reaction progresses, leading to a decrease in the peak intensities of $Ca(OH)_2$ and MgO, and an increase in the content of $MgKPO_4 \cdot 6H_2O$, $Ca_3(PO_4)_2$, $CaCO_3$, and HMC. These changes correlate with improved compressive strength. However, excessive pre-curing duration depletes free water in the system, which hinders CO_2 dissolution and reduces the intensity of carbonate precipitation peaks, thereby negatively affecting the carbon sequestration efficiency.

3. CONCLUSIONS

Through systematic investigation of the effects of the Mg/P ratio, water-to-binder ratio, pre-curing duration, and type and dosage of mineral admixtures on the performance of magnesium potassium phosphate (MPP)-based carbon sequestration materials, the optimal mix proportion was determined. This provides a foundation for subsequent research on the influence of carbonation conditions on the behavior of MPP-based materials.

(1) The compressive strength of magnesium phosphate-based carbon sequestration materials initially increased and then decreased with rising Mg/P ratio. The maximum compressive strength under both ambient and carbonation curing was achieved at an Mg/P ratio of 3:1. At this ratio, the excess MgO serves as a magnesium source for carbonation, making an Mg/P of 3:1 the optimal choice.

(2) With the Mg/P ratio fixed at 3:1, the highest compressive strength was observed at a water-to-binder ratio of 0.25. This ratio promoted sufficient hydration, resulting in a higher formation of hydration products and a more stable pore structure. Thus, the optimal water-to-binder ratio is determined to be 0.25.

(3) Specimens incorporating 10 wt% carbide slag (CCR) exhibited superior compressive strength under both ambient and carbonation curing after 1, 3, and 7 days of pre-curing compared to other mixtures. The carbonation rates at these pre-curing durations were increased by 131.84%, 133.25%, and 109.51%, respectively, relative to the control group (Ctrl). Therefore, the optimal admixture is identified as carbide slag at 10 wt%, and the recommended pre-curing duration is 3 days.

REFERENCES

[1] Soudée E, Péra J. Mechanism of setting reaction in magnesia-phosphate cements. Cement and Concrete Research. 2000; 30(2):315-321.

[2] Wagh AS, Jeong SY. Chemically bonded phosphate ceramics: I, A dissolution model of formation. Journal of the American Ceramic Society. 2003; 86(11):1838-1844.

[3] Mo L, Lv L, Deng M, et al. Influence of fly ash and metakaolin on the microstructure and compressive strength of magnesium potassium phosphate cement paste. Cement and Concrete Research. 2018; 111:116-129.

[4] Liu R, Liu S, Sun S, et al. Medical waste incineration fly ash-based magnesium potassium phosphate cement: Calcium-reinforced chlorine solidification/stabilization mechanism and optimized carbon reduction process strategy. Journal of Environmental Management. 2024; 357:120749.

[5] Chen Z, Liu Y, He B, et al. Role of ammonium citrate in the preparation of high-strength carbonated steel slag cementitious materials. Construction and Building Materials. 2024; 422:135612.

[6] Liang X, Li M, Wang L, et al. Effect of microwave pretreatment on the properties and microstructure of low-concentration carbon dioxide early cured cement-based materials. Buildings. 2024; 14(4):

[7] Wu B, Gevaudan JP, Xiang Y, et al. Novel insights into the amorphous feature of granulated blast furnace slag-supplemented magnesium potassium phosphate cement and its effect on bulk properties. Construction and Building Materials. 2024; 425:135958.

[8] Guan Q, Ma Y, Jin M, et al. Carbonation curing of belite-rich cement: The role of fly ash and strengthening mechanism. Cement and Concrete Composites. 2024; 149:105530.

[9] Cui Y, Wang Y, Li H, et al. A study on particle size of slag on properties of magnesium potassium phosphate cement.

[10] Xu S, Xu C, Dong C, et al. Effect of carbonation curing time on mechanical properties of ecological porous concrete. New Building Materials. 2024; 51(4):92-95 (in Chinese).

[11] Gharsallah S, Khitouni N, Mallah A, et al. Advancing in cesium retention: Application of magnesium phosphate cement composites. Materials. 2024; 17(9): [Article Number].

[12] Lin Z, Zhang L, Zheng W, et al. Properties and interfacial performances with magnesium phosphate cement of coir fiber treated by an efficient water bath method: Effect of immersion temperatures and times. Construction and Building Materials. 2024; 429:136443.

[13] Shi F. Study on mechanical and deformation characteristics of carbonated MgO-carbide slag stabilized soil. Anhui University of Science and Technology. 2024 (in Chinese).

[14] Liang Y, Liu W, Zhao K, et al. Effect of different curing regimes on steel corrosion in alkali-activated slag concrete under accelerated carbonation. Materials Reports. 2024; 38(11):162-169 (in Chinese).

[15] Zhong K, Liu Z, Wang F. Preparation and properties of steel slag powder 3D printing materials via carbonation curing. Materials Reports. 2024; 38(14):173-180 (in Chinese).

[16] Liu Y, Chen Z, Ni H, et al. High-temperature properties of fly ash and silica fume composite magnesium potassium phosphate cement. Construction and Building Materials. 2024; 441:137487.

[17] Qin L, Xie Q, Yang J, et al. Effect of coal fly ash and CO2 curing on performance of magnesium potassium phosphate cement. Journal of CO2 Utilization. 2024; 86:102921.